RSC Advances

ROYAL SOCIETY OF CHEMISTRY

www.rsc.org/advances

Journal Name

ARTICLE

Energetic Interpenetrating Polymer Network Based on Orthogonal Azido-Alkyne Click and Polyurethane for Potential Solid Propellant

Abbas Tanver,[a] Mu-Hua Huang,*[a] Yunjun Luo,*[a] Syed Khalid[a] and Tariq Hussain[b]

Received 00th January 20xx,
Accepted 00th January 20xx

DOI: 10.1039/x0xx00000x

www.rsc.org/Advances

High energetic propellants with synergistic mechanical strength are the prerequisites for aerospace industry and missile technology; though glycidyl azide polymer (GAP) is a renowned and a promising energetic polymer which shows poor mechanical and low-temperature properties. In order to overcome these problems, a novel energetic interpenetrating polymer network (IPN) of Acyl-terminated glycidyl azide polymer (Acyl-GAP) and hydroxyl terminated polybutadiene (HTPB) is effectively synthesized and characterized via an *"in situ"* polymerization by triazole and urethane curing system respectively. Acyl-GAP and Dimethyl 2, 2-di (prop-2-ynyl) malonate (DDPM) have been synthesized and well characterized by using FT-IR, ^{1}H NMR, ^{13}C NMR and GPC. The maximum tensile strength ~ 5.26 MPa and elongation 318 % are achieved with HTPB-PU/Acyl-GAP triazole in 50:50 weight ratios. The solvent resistance properties have been investigated by the equilibrium swelling method and the glass transition temperature (T_g), morphology and thermal stability are evaluated by DSC, SEM and TGA-DTG respectively. Thus, HTPB-PU/Acyl-GAP triazole is a futuristic binder for the composite solid propellant.

Introduction

Interpenetrating polymerization signifies an innovative approach to elucidate the problem of polymer incompatibility. IPN can be elaborated as special class of polymers, which is a combination of two or more polymers in which one is synthesized or polymerized in the presence of others.[1,2] IPN is a useful method to develop a product with more excellent physico-mechanical properties than the normal polyblends. IPN is also known as the polymer alloys and it is one of the fastest emerging areas of research in the field of polymer blends since last two decades.[3] There are two kinds of methodologies, namely sequential and simultaneous polymerization. Sequential IPNs are generally prepared in which the second component network is formed following the formation of first component network. Simultaneous IPNs result from two individual curing processes that occurred at the same time.[4-10] There are also other types of IPNs such as semi, grafted, latex, gradient and thermoplastic IPNs. Semi IPNs have only one component cross-linked, whereas grafted IPNs have covalent cross-links between both networks.[11,12] IPNs with special characteristics have found many interesting applications, such as coating materials,[13] high strength materials,[11] pH-sensitive hydrogels,[14] and biocompatibility materials.[15]

Recent advances in the field of propellant for high energetic properties, GAP is one of the promising binders for propellant industry and many researchers have reported its synthesis, performances and different applications.[16-20] Although GAP has numerous advantageous like high positive heat of formation, higher density and good compatibility with advanced oxidizers like hydrazinium nitroformate (HNF) and ammonium dinitramide, GAP does not show excellent mechanical properties especially low temperature properties due to its poor polymer backbone flexibility.[20] The critical temperature of GAP is 6 °C where the polymeric binder starts to quickly lose its elastomeric properties. Glass transition temperature of GAP are much greater than those of inert binder HTPB and this significantly limits its application in composite solid propellants.[21] Normally, the polymeric binder features can significantly influence the structural integrity of the propellant and can be altered effectively to adjust the mechanical properties of the propellant for specific applications. HTPB is widely used as polymeric binder in composite propellant technology due to its unique physico-chemical properties.[22-27] HTPB exhibits low glass transition temperature, hydrolytic stability, high flexibility and resistance to solvents are excellent properties for the composite solid propellant.[28,29]

In order to make full use of benefits of GAP and HTPB, many attempts have been carried out. However it is significantly inhibited by the poor compatibility between HTPB and GAP due to non polar nature of HTPB and polar nature of GAP.[30] The cross-linked copolymer of HTPB and GAP was synthesized showed two glass transition temperatures at -74.03 °C and -35.84 °C, while the decomposition pattern was similar as observed in their homopolymers. Due to the reactivity differences of terminal hydroxyl groups of GAP and HTPB with different isocyanates, it has been reported that the GAP-HTPB cross-linked networks showed improved mechanical properties over the virgin network of HTPB or GAP.[31] Single glass transition was seen with 30 % of GAP without phase separation while beyond 50 % GAP ratio, no significant effect seen on mechanical properties improvement due to poor miscibility, leading to phase separation. Mathew et al. have

[a] School of Materials Science and Engineering, Beijing Institute of Technology, Beijing, 100081, China
[b] School of Mechatronical Engineering, Beijing Institute of Technology, Beijing, 100081, China
E-mail: yjluo@bit.edu.cn; mhhuang@bit.edu.cn
Electronic Supplementary Information (ESI) available: [details of any supplementary information available should be included here]. See DOI: 10.1039/x0xx00000x

reported maximum mechanical strength around 4.2 MPa and elongation < 200 with 30 % GAP-MDCI in GAP-HTPB cross-linked networks.[31] Bing et al. have claimed 3.83 MPa tensile strength and 593 % elongation by using GAP-HTPB blend binders with 50:50 weight ratios.[32]

Instead of traditional isocyanate curing system, Chinese researcher Ding et al. adopted the triazole curing system based on HTPB and GAP.[33] Blend of propargyl-terminated polybutadiene (PTPB) with GAP under the catalysis of cuprous chloride Cu (I) showed the maximum mechanical strength up to 2.5 MPa and elongation around 50 % when the molar ratios of N_3 versus C≡C was 2.0. It was a good endeavour in order to overcome the miscibility problem of the binders and compatibility issues of the high energy ingredients in the binder system.[33] 1, 3–dipolar cycloaddition between azides and alkynes (Huisgen reaction) is one of the classical click reaction due to the fact that it is virtually quantitative, insensitive, very robust and orthogonal ligation reaction.

One of the finest ways to modify the characteristics of the polymers in order to attain the specific properties is the chemical or physical combination of polymers.[34] Many researchers have employed HTPB with other polymers in order to increase the mechanical strength, thermal stability and chemical resistance. HTPB-PU/Poly (methyl methacrylate) and HTPB-PU/Polystyrene, HTPB-PU/Poly (ethylene oxide) based IPNs have been examined.[35-40] Min et al. investigated the block copolyurethane binder matrices of GAP/Polyethylene glycol and GAP/Polycaprolactone for better mechanical strength.[41]

In the present research, we have developed an energetic IPN which is formed from the cross-linking of two binders system in which one binder (GAP) is highly energetic compared with the other (HTPB). Based on the pioneering work done in the HTPB and GAP system, we wonder if an IPN structure via orthogonal curing reaction will enhance the properties of resulting material. In order to improve the mechanical properties of IPN for potential solid propellants, we designed the networking polymer based on the following considerations: 1, construct of new IPN structure. In the literature, GAP was used directly, which will cure with isocynate, compete with HTPB. If the terminal hydroxyl group of GAP was blocked by O-acylation, it would not react with isocyante, and only pendant azido group of GAP reacted with dialkyne. 2, layer by layer curation of Acyl-GAP and HTPB with different curing agents can improve the mechanical strength as well as thermal properties with IPN formation.

We first synthesized the Acyl-GAP by acetylation of GAP with acetic anhydride catalyzed by 4-(dimethyl amino) pyridine (DMAP). The reason for end capping of terminal hydroxyl groups of GAP with acetyl groups is to allow the highly selective curation through azido groups with dipolarophile curing agent like DDPM. DDPM[42] was also synthesized and characterized by FT-IR, ^{1}H NMR, ^{13}C NMR and GPC. *In situ* polymerization technique was adopted in order to prepare the Acyl-GAP/HTPB IPNs. Triazole cross-linked network of Acyl-GAP was obtained by the reaction of azido group with DDPM while polyurethane network was prepared by the reaction of hydroxyl group of HTPB with isocyanate group of Desmodur N-100 polyisocyante and isophorone diisocyanate (IPDI) mixed curative system as shown in scheme 1. IPNs with different weight ratios of Acyl-GAP and HTPB have been tried; 50:50 weight ratio results the excellent mechanical properties. Thermal studies depict the inward shifting of T_g and more thermally stable networks. SEM studies also revealed the entanglements of networks in HTPB-PU/Acyl-GAP triazole system.

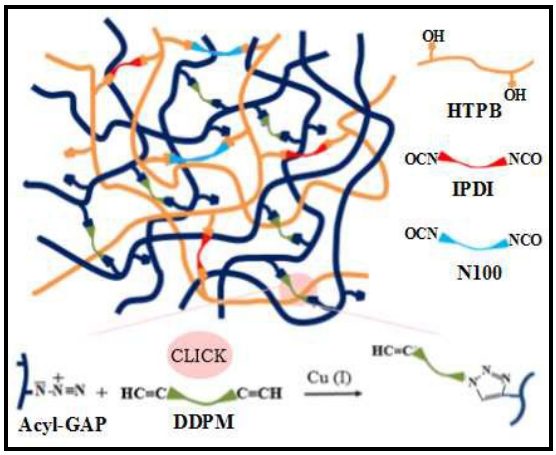

Scheme 1: Schematic representation of click chemistry reaction and IPN structure of Acyl-GAP triazole and HTPB-PU

Experimental

Materials

GAP having molecular weight 3700 g mol^{-1} and hydroxyl contents 29.15 mg KOH g^{-1}, Nitrogen contents, water contents and functionality are 41.3 %, 0.217 % and 1.92 respectively. HTPB molecular weight and hydroxyl contents are 3020 gmol^{-1} and 0.73 mmol g^{-1} respectively, Hydrogen peroxide (H_2O_2) contents, water contents and functionality are 0.022 %, 0.015 % and 2.205 respectively. GAP and HTPB were taken from Liming Research Institute of Chemical Industry, Henan China and was used after vacuum dried for 3 hours at 80 ^{0}C. Isophorone diisocyanate (IPDI) having average molecular weight 222.2 and 9.0009 mmol of NCOper gram of IPDI was taken from Beijing chemical plant. Dibutyl tindilurate (DBTDL) 0.5 % solution in diisooctyl sebacate (DOS) was used and taken from Beijing chemical plant also. Dimethyl malonate and propargyl bromide (80 wt. % in toluene, ca. 9.2 molL^{-1}) were purchased from Aladdin Corporation, Shanghai China. Sodium hydride (70 wt. % dispersion in mineral oil) and ammonium chloride were also purchased from the same. Tetrahydrofuran (THF, AR), petroleum ether, ethyl acetate (EtOAc) and an anhydrous magnesium sulphate were purchased from Sinopharm Chemical Reagent Co. Ltd. (China). Dichloromethane, 4-Dimethyl amino pyridine (DMAP) and Triethylamine were purchased from the Sigma-Aldrich and used as received.

Synthesis of Acyl-Terminated GAP

Acyl-GAP was synthesized by the reported procedure somewhere else with some modification.[43] Approximately to a solution of GAP (2.216 g, 1.15 mmol) and acetic anhydride (0.21 ml, 2.29 mmol) in dry CH_2Cl_2 (3 mL) was added triethylamine (0.32 ml, 2.29 mmol) and DMAP (61 mg, 0.50 mmol) in dry CH_2Cl_2 (2 mL) drop wise at 0 ^{o}C. The resulting reaction mixture was stirred at room temperature overnight. The reaction was quenched by adding water, solvent was removed in vacuum and residue was dissolved in EtOAc (20 mL), which was washed with water and 0.1 N HCl. The aqueous layer was extracted with EtOAc 3 times; combined organics were dried (over $MgSO_4$) and concentrated to give the Acyl-GAP (94 %). Figure 1-C shows the FTIR spectrum and Figure S1 and S2 (Supporting Information) show the ^{13}C NMR and ^{1}H NMR of the Acyl-GAP respectively.

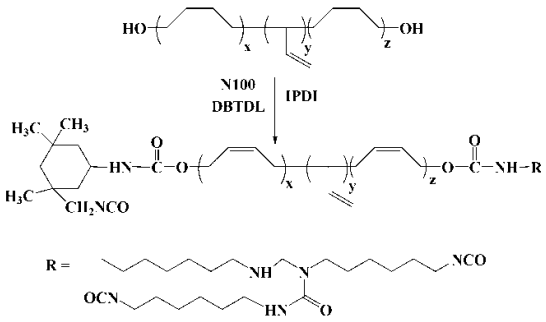

Scheme 2: Schematic illustration for the reaction of HTPB with IPDI and N100.

Synthesis of Dimethyl 2, 2-di (prop-2-ynyl) malonate (DDPM)

A solution of dimethyl malonate (2.5 mL) in 20 mL of THF was added drop wise into the three-neck round bottom flask equipped with reflux condenser, thermometer and magnetic stirrer already contained solution of sodium hydride (1.71g) in 20 mL of THF. The whole mixture reacted for one hour at room temperature and then solution of propargyl bromide (5.1 mL) in 50 mL of THF were added drop wise and allowed to reflux for 3 hours at 110 ^{o}C.[42] Organic layer was extracted with the 50 mL of saturated ammonium chloride and residual organic layer was extracted with 50 mL of diethyl ether three times each. The combined organic were dried over anhydrous $MgSO_4$ and after rotary evaporation, a light yellow solid was obtained which was recrystallized with petroleum ether/ EtOAc (volume ratio 4:1) to get the white solid purified product (yield 82.5 %). Figure 1-D shows the FTIR spectrum, Figure S3 and S4 show the ^{13}C NMR and ^{1}H NMR of the DDPM respectively.

Preparation of single networks

All the reagents were dried overnight in a vacuum oven at 60 ^{o}C before use. Polyurethane network were prepared by mixing the stoichiometric amount of HTPB, IPDI and N100 in a beaker followed by degassing in a vacuum oven at 40 ^{o}C and reaction flow chart is shown in scheme 2. The equivalent ratio of NCO/OH was used as 1.1 and IPDI/N100 weight ratio was 1.0. The required amount of DBTDL (0.3 %) was added as a curing catalyst. The mixture was finally degassed in a vacuum oven before poured into a Teflon coated mold. The mold was finally cured at 60 ^{o}C for 4 days.

For the preparation of triazole cross-linked network, required amount of Acyl-GAP and DDPM were dissolved in THF along with Cu (I) 0.1 wt % which acts as a curing catalyst. Mixture was mechanically stirred under nitrogen atmosphere at room temperature for 30 minutes and reaction flow chart is shown in scheme 3. The mixture was condensed in a rotary evaporator and followed by degassing in a vacuum oven. The reaction mixture was casted into a Teflon mold and cured at 60 ^{o}C for 2 days. Weight ratios of DDPM from 5 to 15 % were used against Acyl-GAP. All triazole cross-linked networks were prepared by controlling the ratio of dipolarophile containing alkynes based on the amount of azido groups.

Synthesis of interpenetrating polymer network (IPNs)

The Acyl-GAP/HTPB IPNs were synthesized by an *in situ* polymerization method where all the reactants, curing agents and catalysts were mixed together (same proportions for each network as indicated in a single network preparation). A series of Acyl-GAP/HTPB IPNs were prepared by changing the relative amount of

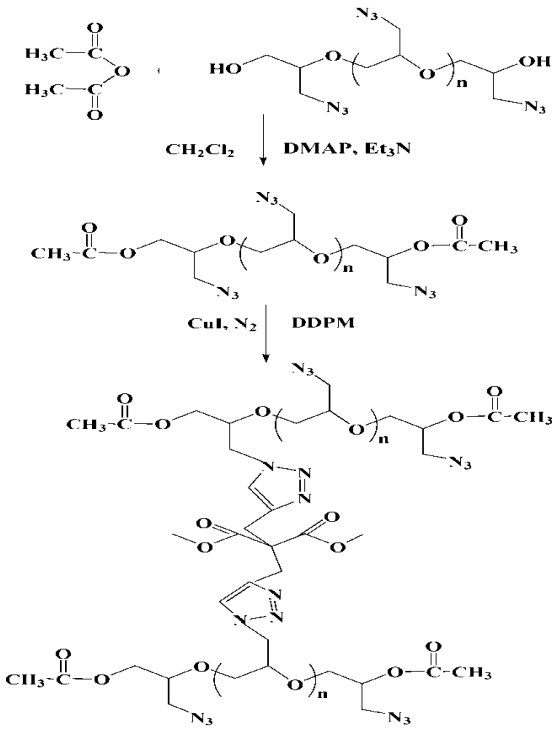

Scheme 3: Schematic illustration for the synthesis of Acyl-GAP and reaction of Acyl-GAP with DDPM

Acyl-GAP weight proportions (90, 70, 50, 30, 10 wt. %) with respect to HTPB. The required amount of Acyl-GAP and DDPM were dissolved in THF, HTPB along with IPDI and N100 were also added into the reaction mixture. Finally the DBTDL and Cu (I) were added and the mixture was mechanically stirred under nitrogen atmosphere at room temperature for 30 minutes. The resultant mixture was condensed by rotating evaporation and casted into the Teflon coated mold. All IPNs films were vacuum-dried and cured at 60 ^{o}C for 4 days. In this study, a series of experiments have been performed in order to set the catalytic amount for triazole and polyurethane network formation. Finally 0.3 % of DBTDL concentration for polyurethane network and 0.1 wt. % of Cu (I) for triazole cross-linked network were selected.

Characterization

Fourier transform infrared spectroscopy (FTIR) measurements were recorded (Nicolet FTIR-8700, Thermo) in the range of 4000-500 cm^{-1}, ^{1}H NMR and ^{13}C NMR spectra of Acyl-GAP and DDPM were obtained out using a Varian mercury-plus 400 MHz nuclear magnetic resonance (NMR) spectrometer in $CDCl_3$ solution using tetramethylsilane as internal standard. Gel permeation chromatography GPC was carried out on a (GPC; LC-20A, Shimadzu) at 40 ^{o}C using THF as the mobile phase and the flow rate was 1 mL/min. Polystyrene was used as standard for calibration.

Differential scanning calorimetric (DSC) analysis was carried out on Mettler Toledo DSC1 over a temperature range of -100 to 50 ^{o}C with heating rate of 10 ^{o}C/min under nitrogen flow of 40 mL/min. 2-3 mg of each sample was taken in small aluminum cell. Thermo gravimetric analysis was performed using TGA analyzer (TGA/DSC1SF/417-2, Mettler Toledo) with heating rates of 10 ^{o}C/min under nitrogen flow of (40 mL/min) from room temperature to 600 ^{o}C. The mechanical parameters, including

tensile strength (σ_b) and elongation at break (ε_b) of all the dumb bell shape samples were measured on universal testing machine (Instron-6022, Shimadzu Co., Ltd.) with a constant rate of 100 mm/min and mean values of five samples were taken. Scanning electron microscope (SEM) S-4800 (Hitachi) was used in order to study the surface morphology. All samples were fractured with liquid nitrogen and after gold sputtering, microphotographs were taken.

The number average molecular weight (Mn), weight average molecular weight (Mw) and poly dispersity index values (PDI= Mw/Mn) of the GAP and Acyl-GAP are shown in table S1. The Mn of GAP and Acyl-GAP was obtained 4783 and 4825 g/mol respectively while the Mw were 7193 and 7331 g/mol respectively. A PDI value of GAP and Acyl-GAP was achieved 1.504 and 1.5193 respectively. Increase in average molecular weight was due to partial extension in chain due to acetylation of GAP.

The impact sensitivity as well as the friction sensitivity of Acyl-GAP, PU, triazole and IPN's were measured. The impact sensitivity was measured with a 5 kg drop weight using a BAM drop weight apparatus. The results are based on tests on both sides of the 50 % probability level using the up-and-down method. The friction sensitivity was measured with a BAM friction apparatus by applying a thin film to a ceramic tile and lowering the friction apparatus arm. The weight was placed on the outer groove of the arm, by pressing the button, dragging ceramic pellet across the sample. The sample was observed for any sign of ignition, spark or smoke and repeated six times by changing the mass. The results of these tests are given in Table S4 (Supporting information).

Results and Discussion

Acyl-GAP was synthesized by the acetylation of GAP with DMAP, triethylamine and acetic anhydride in CH_2Cl_2. Figure 1 shows the FTIR spectrum of GAP, Acyl-GAP, Acyl-GAP/DDPM cured film and Acyl-GAP/HTPB cured film. Figure 1-B depicts that the main characteristic peaks at about 1283 and 2102 cm^{-1} corresponds to the $-N_3$ of GAP, asymmetric and symmetric $-CH_2$ and -CH stretching peaks between 2926 and 2874 cm^{-1} while broad intense stretching vibrations of OH and C-O-C of GAP at about 3300-3500 cm^{-1} and 1120 cm^{-1} respectively. Figure 1-C shows the FTIR spectrum of Acyl-GAP, compared with the spectrum of GAP 1-B, besides the main peaks, a new strong band at 1740 cm^{-1} clearly specifies the C=O stretching frequency and disappearance of broad OH peak after acetylation of GAP.

As shown in Figure 1-D and E, the peak located at 3291 cm^{-1} which was assigned to ≡CH stretching vibration of alkynyl group of DDPM disappeared in the Acyl-GAP/DDPM cured film, however the peak at 2102 cm^{-1} as a result of azido groups remains in the spectrum due to excess in nature. FTIR spectrum of Figure 1-A and F shows HTPB and Acyl-GAP/HTPB cured film. As shown in Figure S2 (Supporting information), ^{1}H NMR spectrum of Acyl-GAP has a peak at around 3.8 ppm due to protons of polyether main chain of GAP attributed to $-CH_2$, -CH and 3.4 ppm ascribed to the $-CH_2N_3$. New peak observed after acetylation at around 2.11 ppm is attributed to CH_3. Figure S1 (Supporting information), depicts ^{13}C NMR spectrum of Acyl-GAP, appearance of new peak at 163 ppm is ascribed to the carbonyl carbon and peak at 22 ppm is attributed to the $-CH_3$ of the acetyl group. ^{1}H NMR spectrum of DDPM presented three peaks located at 2.1 ppm (2H, c), 3.02 ppm (4H, b) and 3.76 ppm assigned to –CH, $-CH_2$ and $-CH_3$, while ^{13}C NMR spectrum depicts five characteristics peaks at (c) 23.1ppm, (a) 53.6 ppm, (d) 72.07 ppm, (e) 77.46 ppm and (b) 169.4 ppm.

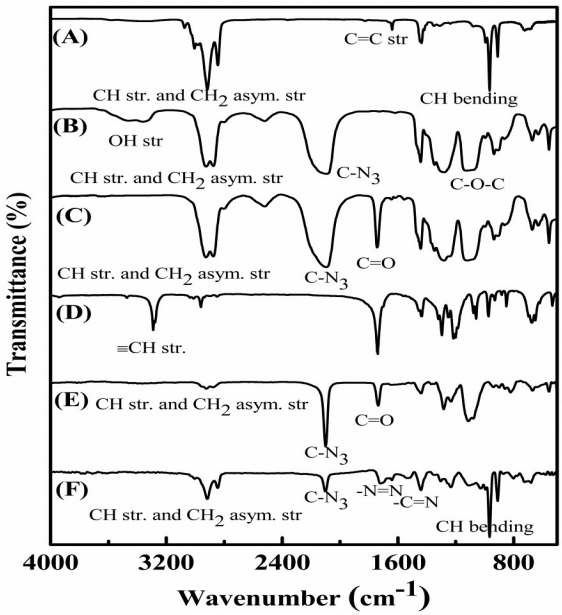

Figure 1: FTIR spectra of (A) HTPB, (B) GAP, (C) Acyl-GAP, (D) DDPM, (E) Acyl-GAP/DDPM, (F) Acyl-GAP/HTPB cured film.

In situ FT-IR kinetic studies of Acyl-GAP/DDPM and HTPB/IPDI-N100

In order to get comprehensive information regarding reaction mechanism, in situ FTIR kinetic study was carried out. Figure S5 (Supporting information) shows the reaction kinetics of polyurethane and triazole network formation in terms of characteristic peaks conversion with respect to time, HTPB network formation kinetics was followed by monitoring the change in intensity of absorption band of NCO stretching at 2258 cm^{-1} and CO stretching at 1730 cm^{-1}. Variations in the height of peaks were calculated with Omnic software. NCO stretching band decreases and finally disappears upon completion of reaction. New absorption peaks at 1731cm^{-1} and 1508 cm^{-1} assigned to CO and NH stretching appeared due to polyurethane formation. While triazole cross-linked network kinetics was followed by observing the change in intensity of ≡CH stretching of alkynyl groups at 3291 cm^{-1} and appearance of new peaks around 1620 cm^{-1} and 1555 cm^{-1} due to –N=N and –C=N respectively,[42] however the peak at 2102 cm^{-1} due to $-N_3$ group remains in the spectrum due to high concentration.

In situ FTIR kinetic studies show that almost 80 % triazole and polyurethane network formation takes place within 20 hours and Figure S5 demonstrates the reaction conversion-time profile. Rate of conversion is very fast and after 80 % conversion, polyurethane reaction slows down and rate of diffusion is greatly reduced and almost 100 % conversion completed in four days. While triazole reaction is very fast as compared to the urethane and 100 % conversion took place in less than 50 hours. This may be due to catalytic amount of Cu (I) and excess of $-N_3$ groups which favours the completion of reaction in short time. The observations as a result of in situ kinetic studies of PU and triazole network formation are very important for defining the IPN conditions.

Cross-linking Densities and Swelling Behaviours of the Acyl-GAP/DDPM Materials

Cross-linking density and the swelling behaviour are important factors to determine the mechanical performance of the material.

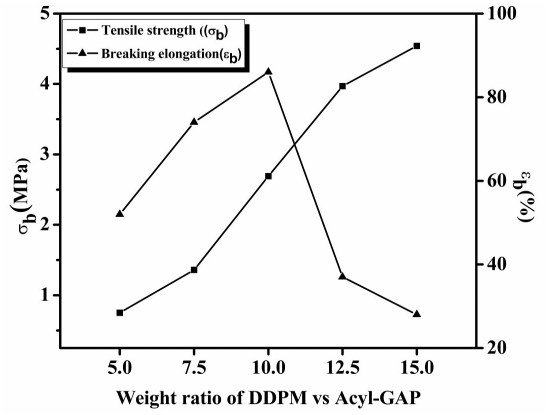

Figure 2: Effect of weight ratio of DDPM vs Acyl-GAP on the tensile strebgth (σ) and breaking elongation (ε_b)

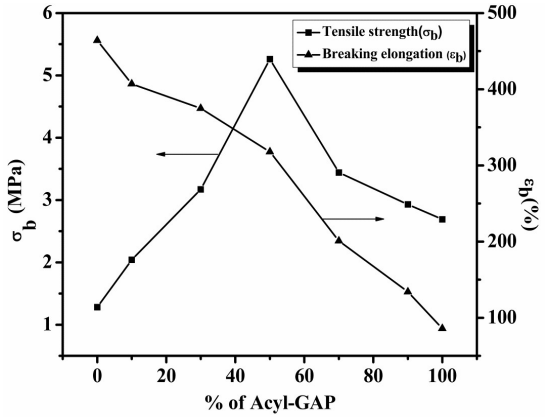

Figure 3: Effect of weight ratio of % Acyl-GAP vs HTPB on the tensile strebgth (σ) and breaking elongation (ε_b)

By changing the weight ratio of Acyl-GAP to DDPM, cross-linking densities were examined. Figure S6 (Supporting information) depicts the effects of weight ratio of Acyl-GAP to DDPM on the swelling degree and cross-linking densities of the as prepared Acyl-GAP/DDPM films. Generally increase in cross-linking points inhibits the swelling behaviour. With the increase in weight ratio of Acyl-GAP to DDPM from 5 to 15 %, cross-linking density increased from 0.42 to the maximum value of 0.78 while the swelling degree decreased from 37 % to the minimum value of 4 %. The weight ratio effect of Acyl-GAP to HTPB on cross-linking density is shown in figure S7. With increase in weight ratio, cross-linking density increase from 0.42 to 0.80 and then decreased. At 50 % of Acyl-GAP, cross-linking density is maximum, beyond this; cross-linking density goes down and reaches up to 0.57 due to maximum steric hindrance. Generally higher cross-linking density results in higher tensile strength and lower elongation at break.[33]

Mechanical Properties

The weight ratio effects of Acyl-GAP to DDPM on tensile strength (σ_b) and breaking elongation (ε_b) of the Acyl-GAP/DDPM films are shown in Figure 2. Increase in weight ratio of DDPM to Acyl-GAP, tensile strength (σ_b) gradually increased from 0.75 to 4.54 MPa while the breaking elongation initially increased up to 86 % and then decreased. This decrease in breaking elongation is due to the higher cross-linked density.[42] As the weight ratio of the DDPM to Acyl-GAP increases from 5 % to 15 %, more and more alkynyl groups took part in triazole linkages and this increase of cross-linking points restricts the deformation, as a result of that tensile strength increased with an expense of breaking elongation. Figure 2 shows that optimum mechanical properties achieved by using 10 % of the DDPM and beyond this ratio although the tensile strength increases but the elongation decreases dramatically due to stiffer network associated to azido side linkage.

Figure 3 depicts the dependence of the mechanical parameters, including tensile strength (σ_b) and elongation at break (ε_b) of the Acyl-GAP/HTPB IPNs. Pure urethane network shows the tensile strength (σ_b) and breaking elongation (ε_b) 1.28 MPa and 464 % respectively, while triazole cross-linked network shows the tensile strength (σ_b) and breaking elongation (ε_b) 2.69 MPa and 86 % respectively. Figure 3 also indicates that by increasing the weight ratio of the Acyl-GAP, tensile strength first increased from 1.28 MPa to 5.26 MPa and then steadily decreased up to 2.69 MPa, but the breaking elongation gradually decreased from 464 % to 86 %, a substantial increase in the tensile strength and decrease in the breaking elongation during in situ polymerization has been observed. It is interesting to report that with 50 % of Acyl-GAP in Acyl-GAP/HTPB IPNs, highest tensile strength of 5.26 MPa with 318 % elongation achieved and this may be ascribed due to the permanent entanglements (catenation) of both cross-linked networks. Due to enhanced interlocking of urethane and triazole networks, chain flexibility is highly restricted and elongation at break is significantly reduced. Beyond 50 % Acyl-GAP, the flexibility of Acyl- GAP is inhibited by the $-N_3$ groups of the side chain and tensile strength and elongation at break progressively drops up to 2.69 MPa and 86 % respectively in pure triazole network. These might be the possible reasons for increase in tensile strength and decrease of elongation at break with the increase of Acyl-GAP. IPNs with more cross-linked structure and stiffness possess higher tensile strength than that of PU and triazole networks individually.

Thermal Studies

Figure 4 depicts the DSC thermo grams of pure PU, triazole and different weight ratios of Acyl-GAP/PU while table 1S (Supporting information) summarized the glass transition temperatures (T_g). The T_g of PU and triazole networks was found to be -77.5 ^oC and -34.5 ^oC respectively. With the increase in weight ratio of Acyl-GAP up to 30 %, only one T_g is observed and also slightly increased from -77.5 ^oC to -72.5 ^oC, this may be due to interlocking of polymer networks and shortening of space among cross-linked points. Although thermo gram with 50:50 % Acyl-GAP/HTPB weight ratio, shows two glass transition temperatures at -75.3 ^oC and -36.9 ^oC

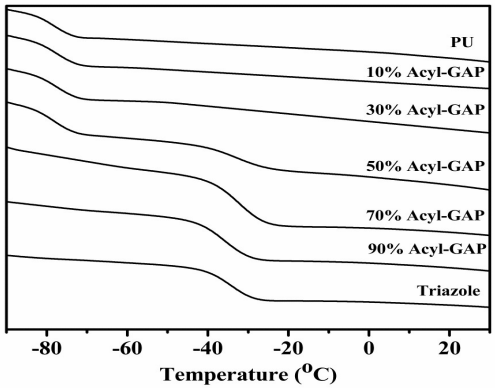

Figure 4: DSC thermo grams of PU, (A) 10 %, (B) 30 %, (C) 50 %, (D) 70 %, (E) 90 % Acyl-GAP and Triazole

this may be due to phase separation but auspiciously having synergistic mechanical properties. Same trend of inward shift of T_g can be seen from 70 % Acyl-GAP to triazole network.

TGA/DTG Analysis

One of the most important tools in the propellant industry is thermal stability of the polymer products. Thermal decomposition is directly related with important performance parameters like heat of explosion, detonation energy and detonation velocity.[44,45] Figure 5 depicts the TGA thermo gram of polyurethane, triazole and PU/Triazole networks. TGA scan of triazole network shows weight loss in two stages. The first stage decomposition of triazole takes place in the temperature range of 190–270 °C with a weight loss of 38 % due to liberation of nitrogen,[17,21] while the second stagedecomposition involves the degradation of polyether main chain of Acyl-GAP in the temperature range of 270– 464 °C. The residue left behind after the decomposition is around 29 %.[31]

HTPB cross-linked network decomposition undergoes in two stages with indistinct separation. The first stage decomposition is in the range of 210– 415 °C with a mass loss of 21 % due to depolymerization, cyclization and partial decomposition of cyclized products. Second stage decomposition is in the range of 415–490 °C due to the dehydrogenation and decomposition of the remaining cyclized products.[46-48] Residue left behind after the complete decomposition is almost 1 %. From thermo gravimetric curves, a better thermal stability can be seen with increasing the weight ratio of Acyl-GAP in PU/Triazole networks. Peak decomposition temperatures of Acyl-GAP, PU, triazole and IPN's are shown in table S3. It can be observed from DTG curves (Fig. 6) that during the first and second stage, peak decomposition temperatures shifted from 248 °C to 253 °C and from 458 °C to 462 °C respectively. Higher the cross-linked network, more energy is required for the decomposition,[33] this trend clearly shows the evidence for thermal stability and compact network formation due to interpenetration and physical entanglement of networks.

TG-FTIR Spectroscopic Studies

To elucidate the thermal decomposition pattern of PU/Triazole cross-linked networks, TG-FTIR is used to identify the constituents of gas products. The 3-D TG-FTIR of the decomposition products are shown in the Figure S8 (Supporting information), while FTIR spectra of the respected gases are presented in the Figure S9. The gas lines

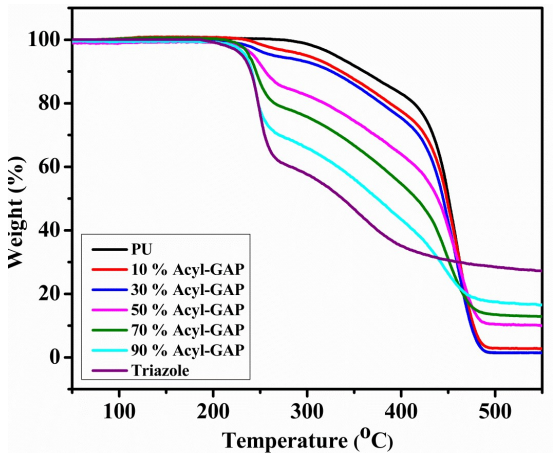

Figure 5: TGA curves of PU, Triazole and different ratios of Acyl-GAP/HTPB

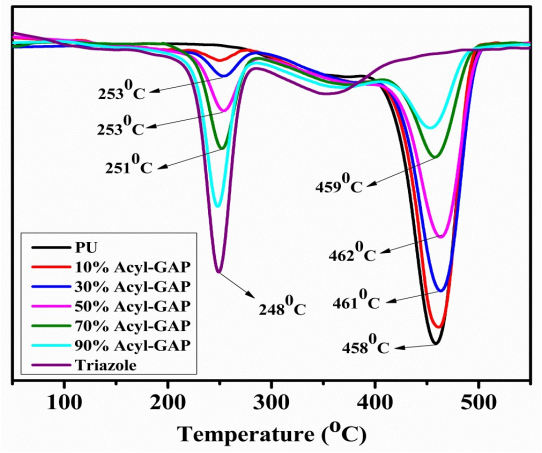

Figure 6: DTG curves of PU, Triazole and different ratios of Acyl-GAP/HTPB

between TGA analyzer and FTIR were heated to 220 °C. Primary evolved gases are due to the decompositions of triazole and polyurethane cross-linked networks. The gas products at 250 °C were identified as CO_2 (2380 and 668 cm^{-1}), N_2O around (2240 cm^{-1}) and HCN (712 cm^{-1}). In addition, the emissions of CH_2O, C_2H_4O or their mixtures (2750-3000 cm^{-1}) were also identified at 460 °C. FTIR spectroscopy does not detect the N_2 and H_2 due to symmetric nature of these gaseous products.

Morphological Studies

Figure 7 depicts the morphologies of fractured surfaces of PU, triazole and HTPB-PU/Acyl-GAP triazole cross-linked networks. Morphological feathers of polyurethane and triazole cross-linked networks are entirely different. Wrinkles and ravines of the fractured surface are prominent in triazole network. SEM micrograph 7-A clearly shows the smooth and glassy microstructures because it was brittle material due to the rigid cross-linked triazole network whereas the micrograph 7-B of the polyurethane exhibits the rough microstructures as compared to the triazole. From the cross sectional surfaces of HTPB-PU/Acyl-GAP Triazole (7-C and 7-D), formation of IPN is vividly seen by the existence of intricate entanglements, wherein, the polymer chains appear to penetrate inward and outward over one another in the polymer matrix showing good compatibility.[49] We also observed micro to nanometer thick long fibers which are crossed and entangled with each other. The inwardly shifting of T_g in DSC and superior mechanical properties of HTPB-PU/Acyl-GAP triazole networks as described earlier is the manifestation of entanglements of both networks.[50]

Conclusion

A novel approach has been adopted in order to fabricate the energetic binder with improved mechanical and thermal properties. Acyl-GAP and DDPM were efficiently synthesized and characterized for triazole curing system and different weight ratios used to get the adequate mechanical characteristics. A series of HTPB-PU/Acyl-GAP triazole cross-linked networks containing 90, 70, 50, 30 and 10 wt. % of Acyl-GAP were synthesized via an *"in situ"* process in which all ingredients were mixed together and the networks were formed independently. The optimum mechanical strength and elongation were achieved with 50:50 HTPB-PU/Acyl-GAP triazole weight ratios.

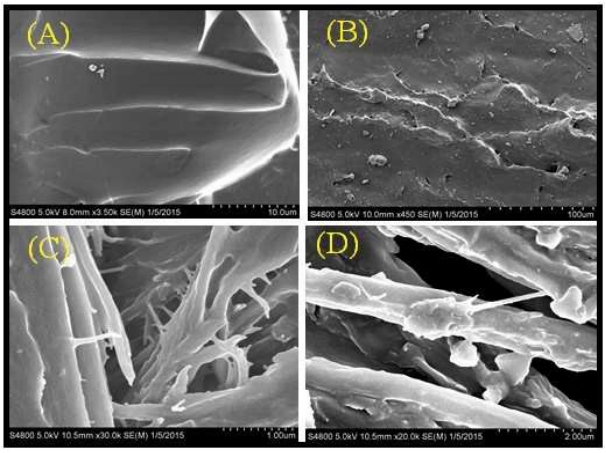

Figure 7: SEM images for the fractured surfaces of the films coded as (A) Triazole, (B) PU, (C) and (D) 50:50 % Acyl-GAP/HTPB

TGA-DTG studies depict the formation of more thermally stable networks and inward shifting of glass transition temperature in DSC which can be solely attributed to the interpenetration of the networks. Morphological studies illustrate that the compact networks are formed by interlocking and physical entanglement of networks.

References

1. Ajithkumar, S.; Patel, N. K.; Kansara, S. S. *Eur. Polym. J.* 2000, **36**, 2387-2393.
2. Chen, S.; Wang, Q.; Wang, T. *Polym. Test.* 2011, **30**, 726-731.
3. Pissis, P.; Georgoussis, G.; Bershtein, V. A.; Neagu, E.; Fainleib, A. M. *J. Non-Cryst. Solids.* 2002, **305**, 150-158.
4. Gitsov, I.; Zhu, C. *J. Am. Chem. Soc.* 2003, **125**, 11228-11234.
5. Jansen, B. J. P.; Rastogi, S.; Meijer, H. E. H.; Lemstra, P. J. *Macromol.* 1999, **32**, 6290-6297.
6. Nakanishi, H.; Satoh, M.; Norisuye, T.; Tran-Cong-Miyata, Q. *Macromol.* 2004, **37**, 8495-8498.
7. Turner, J. S.; Cheng, Y. L. *Macromol.* 2000, **33**, 3714-3718.
8. Abbasi, F.; Mirzadeh, H.; Katbab, A. A. *J. Appl. Polym. Sci.* 2002, **86**, 3480-3485.
9. Fichet, O.; Vidal, F.; Laskar, J.; Teyssie, D. *Polym.* 2005, **46**, 37-47.
10. Turner, J. S.; Cheng, Y. L. *Macromol.* 2003, **36**, 1962-1966.
11. Chaudhary, S.; Parthasarathy, S.; Kumar, D.; Rajagopal, C.; Roy, P. K. *J. Appl. Polym. Sci.* 2014, **131**.
12. Jayasuriya, M. M.; Hourston, D. J. *J. Appl. Polym. Sci.* 2012, **124**, 3558-3564.
13. Gao, D.; Jia, M. *J. Appl. Polym. Sci.* 2013, **128**, 3619-3630.
14. Hu, Y.-Y.; Zhang, J.; Fang, Q.-C.; Jiang, D.-M.; Lin, C.-C.; Zeng, Y.; Jiang, J.-S. *J. Appl. Polym. Sci.* 2015, **132**.
15. Wang, J.-J.; Wu, M.-B.; Xiang, T.; Wang, R.; Sun, S.-D.; Zhao, C.-S. *J. Appl. Polym. Sci.* 2015, **132**.
16. Provatas, A. *A. Energetic Polymers and Plasticizers for Explosive Formulation—A Review of Recent Advances*; DSTO-TR-0966, Defence Science & Technology Organization, Melbourne, Australia, 2000.
17. Selim, K.; Özkar, S.; Yilmaz, L. *J. Appl. Polym. Sci.* 2000, **77**, 538-546.
18. Kasıkçı, H.; Pekel, F.; Özkar, S. *J. Appl. Polym. Sci.* 2001, **80**, 65-70.
19. Murali Mohan, Y.; Padmanabha Raju, M.; Mohana Raju, K. *J. Appl. Polym. Sci.* 2004, **93**, 2157-2163.
20. Manu, S. K.; Varghese, T. L.; Mathew, S.; Ninan, K. N. *J. Appl. Polym. Sci.* 2009, **114**, 3360-3368.
21. Mohan, Y. M.; Raju, K. M. *Des. Monomers Ploym.* 2005, **8**, 159.
22. Davenas, A. *J. Propul. Power.* 2003, **19**, 1108-1128.
23. DeLuca, L. T.; Galfetti, L.; Maggi, F.; Colombo, G.; Merotto, L.; Boiocchi, M.; Paravan, C.; Reina, A.; Tadini, P.; Fanton, L. *Acta Astronaut.* 2013, **92**, 150-162.
24. Abkay, M. K.; Davendra, P. D. *Res. J. Chem. Environ.* 2010, **14**, 94–103.
25. Badgujar, D. M.; Talawar, M. B.; Asthana, S. N.; Mahulikar, P. P. *J. Hazard. Mater.* 2008, **151**, 289-305.
26. Assink, R. A.; Lang, D. P.; Celina, M. *J. Appl. Polym. Sci.* 2001, **81**, 453-459.
27. Hailu, K.; Guthausen, G.; Becker, W.; König, A.; Bendfeld, A.; Geissler, E. *Polym. Test.* 2010, **29**, 513-519.
28. Consaga, J. P.; French, D. M. *J. Appl. Polym. Sci.* 1971, ***15***, 2941-2956.
29. Sekkar, V.; Bhagawan, S. S.; Prabhakaran, N.; Rama Rao, M.; Ninan, K. N. *Polym.* 2000, **41**, 6773-6786.
30. Manu, S. K.; Varghese, T. L.; Mathew, S.; Ninan, K. N. *J. Propul. Power.* 2009, **25**, 533-536.
31. Mathew, S.; Manu, S. K.; Varghese, T. L. *Propellants, Explos., Pyrotech.* 2008, **33**, 146-152.
32. Bing, N. I.; Guang-ming, Q. I. N.; Xiu-lun, R. A. N. *Energ. Mater.* 2010, **18**, 167-173.
33. Ding, Y.; Hu, C.; Guo, X.; Che, Y.; Huang, J. *J. Appl. Polym. Sci.* 2014, 131, 40007.
34. Athawale, V. D.; Raut, S. S. *Eur. Polym. J.* 2002, **38**, 2033-2040.
35. Xie, H.-Q.; Guo, J.-S. *Eur. Polym. J.* 2002, **38**, 2271-2277.
36. Plesse, C.; Vidal, F.; Gauthier, C.; Pelletier, J.-M.; Chevrot, C.; Teyssié, D. *Polym.* 2007, **48**, 696-703.
37. Wang, S. H.; Zawadzki, S.; Akcelrud, L. *J. Polym. Sci., Part B: Polym. Phy.* 2000, **38**, 2861-2872.
38. Roha, M.; Dong, F. *J. Appl. Polym. Sci.* 1992, **45**, 1397-1409.
39. Jia, D. M.; You, C. J.; Wu, B.; Wang, M. Z. *Int. Polym. Process.* 1988, **3**, 205-210.
40. Han, M. H.; Kim, S. C. *Polym. Adv. Technol.* 1997, **8**, 741-746.
41. Sun Min, B. *Propellants, Explos., Pyrotech.* 2008, **33**, 131-138.
42. Hu, C.; Guo, X.; Jing, Y.; Chen, J.; Zhang, C.; Huang, J. *J. Appl. Polym. Sci.* 2014, **131**, 40007.
43. Xu, S.; Held, I.; Kempf, B.; Mayr, H.; Steglich, W.; Zipse, H. *Chem. - Eur. J.* 2005, **11**, 4751-4757.
44. Herder, G.; Weterings, F. P.; de Klerk, W. P. C. *J. Therm. Anal. Calorim.* 2003, **72**, 921-929.
45. Krabbendam-La Haye, E. L. M.; de Klerk, W. P. C.; Miszczak, M.; Szymanowski, J. *J. Therm. Anal. Calorim.* 2003, **72**, 931-942.
46. Ninan, K. N.; Krishnan, K.; Rajeev, R.; Viswanathan, G. *Propellants, Explos., Pyrotech.* 1996, **21**, 199-202.
47. Chen, J. K.; Brill, T. B. *Combust. Flame.* 1991, **87**, 217-232.
48. Simon, J.; Bajpai, A. *Eur. Polym. J.* 2003, **39**, 2077-2089.
49. Desai, S.; Thakore, I. M.; Brennan, A.; Devi, S. *J. Appl. Polym. Sci.* 2002, **83**, 1576-1585.,
50. Shyu, S. S.; Chen, D. S.; Lai, J. Y. *J. Appl. Polym. Sci.* 1987, **34**, 2151-2162.
51. Miró Sabaté, C.; Delalu, H.; Jeanneau, *Chemistry – An Asian Journal* 2012, **7**, 1085-1095.